

# Resistance behavior near the magnetic-field-tuned quantum transition in superconducting amorphous In–O films

V.F. Gantmakher\*, M.V. Golubkov, V.T. Dolgopolov, G.E. Tsydynzhapov, and A.A. Shashkin  
*Institute of Solid State Physics, Russian Academy of Sciences, 142432 Chernogolovka, Russia*

We have studied the magnetic-field-tuned superconductivity destroying quantum transition in amorphous In–O films with the onset of superconductivity in zero field at about 2 K. At temperatures down to 30 mK the critical resistance  $R_c \equiv R(T, B_c)$  has been found to change approximately linearly with temperature, which is in contradiction to a standard description where zero slope  $\partial R_c/\partial T = 0$  is assumed near  $T = 0$ . To make the data  $R(T, B)$  collapse in the vicinity of transition against scaling variable  $(B - B_c)/T^{1/y}$ , one has either to allow for the intrinsic temperature dependence of  $R_c$  or to postulate the critical field  $B_c$  to be temperature-dependent  $\Delta B_c = B_c(T) - B_c(0) \propto T^{1+1/y}$ . We find that the state on the high-field side of the transition can be both insulating and metallic and we determine the critical index  $y \approx 1.2$ .

PACS numbers: 05.70 Fh, 74.20 Mn, 74.25 Dw

## I. INTRODUCTION

The class of quantum phase transitions (QPT) includes a field-induced superconductor–insulator transition (SIT) in two-dimensional (2D) disordered superconductors proposed by Fisher [1]. Fisher argued that the magnetic field alters a superconducting state of a disordered film at low fields, through a metallic one with the universal sheet resistance  $R_{\text{un}}$  close to  $h/4e^2 \simeq 6.4 \text{ k}\Omega$  at the critical field  $B = B_c$ , to an insulating state at fields  $B > B_c$ . The SIT is supposed to be continuous with the correlation length  $\xi$  diverging as  $\xi = \xi_0(B - B_c)^{-\nu}$ , where the critical index  $\nu > 1$ . It was argued theoretically [2] and confirmed experimentally for amorphous films [3,4] that the dynamical critical index  $z$ , which determines the characteristic energy  $U \sim \xi^{-z}$ , is equal to  $z = 1$ . At finite temperatures, when plotted against scaling variable  $u$ ,

$$u = (B - B_c)/T^{1/y}, \quad y = z\nu, \quad (1)$$

all data  $R(T, B)$  near the transition point  $(0, B_c)$  should fall on a universal curve [1]

$$R(T, B) \equiv R_c r(u), \quad r(0) = 1. \quad (2)$$

Experimental studies [3,4] demonstrated the collapse of  $R(T, B)$  as a function of  $u$  and apparently supported this model. Still, these raise some questions. In the high-magnetic-field limit, amorphous Mo–Ge films from Ref. [4] displayed only 5% increase of the resistance with ten-fold decrease of temperature and behaved like a metal with small quantum corrections to the resistance. On In–O films the quasireentrant scenario was observed [3]: at fields below  $B_c$ , the derivative  $\partial R/\partial T$  was positive near the superconducting transition temperature  $T_c$  but became negative at lower temperatures (see below, next section).

Here, we perform the detailed study on amorphous  $\text{In}_2\text{O}_x$  ( $x < 3$ ) films looking for experimental evidence

as concerns unclear aspects of the Fisher transition. The main question is whether the field-induced phase transition in amorphous  $\text{In}_2\text{O}_x$  films is indeed a continuous QPT at zero temperature [5] or a broadened thermodynamic transition with temperature-dependent critical field  $B_{c2}(T)$  as known from the theory of superconductivity. A principal argument in favour of QPT would be the scaling relations, i.e.,  $R(T, B)$  should take the form (2).

The scaling relations have two constituents. First, the derivative on the isomagnetic curve  $R(T, B_c)$  at  $T = 0$  should equal zero [1]:

$$R(T, B_c) \equiv R_c(T) = R_c (1 + O(T^2)), \quad \left. \frac{\partial R}{\partial T} \right|_{(0, B_c)} = 0. \quad (3)$$

This implies that isotherms  $R(B) \Big|_{T=\text{const}}$  intersect at the same point  $(B_c, R_c)$  for all  $T$  in the scaling region. Expanding the isotherms  $R(B)$  in the vicinity of  $B_c$

$$R(B) = R_c + \left( \frac{\partial R}{\partial B} \right)_{B_c} (B - B_c) \quad (4)$$

we get from Eq. (2) the second component of the scaling relations

$$\left( \frac{\partial R}{\partial B} \right)_{B_c} \propto T^{-1/y}. \quad (5)$$

From Eqs. (4,5) it follows that near the transition point  $(0, B_c)$  the universal curve is a linear function

$$r(u) = 1 + \beta u. \quad (6)$$

The procedure of experimental tests is defined by Eqs. (3) and (5). One has to find either the isomagnetic curve with zero slope near  $T = 0$  or the crossing point of low-temperature isotherms to derive  $B_c$  and  $R_c$ . The value of  $y$  is determined from the temperature dependence of the

derivative (5). The last step is to determine the scaling region from plot (2).

We intend to use this procedure for samples that are farther from the zero-field SIT as compared to Ref. [3]. In amorphous  $\text{In}_2\text{O}_x$  films the carrier density  $n$  can be decreased (increased) by increasing (decreasing) the oxygen content; the process is reversible provided the material remains amorphous (experimental details are discussed in the next section, together with the role of granularity). As the density  $n$  increases, the sample shifts deeper into the superconducting region. This leads to increasing the conductance of the high-field state, which is expected in theory [1] to be insulating, and the superconducting transition temperature  $T_{c0}$  at zero field, and the critical magnetic field  $B_c$ . As a result, one may expect to find the fingerprints of an ordinary thermodynamic transition that certainly exists somewhere very deeply in this region. It is shown in section III that shifting inward the superconducting region gives rise to the appearance of a linear term in Eq. (3) so that the scaling representation (2) fails. Nevertheless, this can be restored in generalized form if we compensate for the linear term in  $R$  by introducing the temperature dependence of either  $B_c$  in Eq. (1) or  $R_c$  in Eq. (2). In this way we confirm that the field-tuned quantum SIT does occur in our films.

In section IV we analyze whether the observed QPT is the one described by Fisher [1] or it belongs to a more general group. We demonstrate that (i) the critical resistivity  $R_c$  depends on carrier density; (ii) the high-field state can be metallic as well as insulating; and (iii) the reduced dimension is not of crucial importance. In particular, the film magnetoresistance is not very sensitive to the magnetic field direction. The obtained data on zero-temperature QPTs are summarized to form a phase diagram. We conclude that for field-tuned quantum SIT a strong disorder is important.

## II. EXPERIMENTAL

### A. Samples and measurements

The experiments were performed on amorphous In–O films, 200 Å thick [6]. Such a material proved to be very useful for investigations of the transport properties near the SIT [3,7–12]. Oxygen deficiency compared to fully stoichiometric insulating compound  $\text{In}_2\text{O}_3$  causes the film conductivity. By changing the oxygen content one can cover the range from a metallic superconducting material to an insulator with activated conductance [7]. The procedures to change the film state are described in detail in Refs. [11,12]. To reinforce the superconducting properties of our films and to increase  $T_{c0}$  we used heating in vacuum up to a temperature from the interval 70 – 110°C until the sample resistance saturated or even

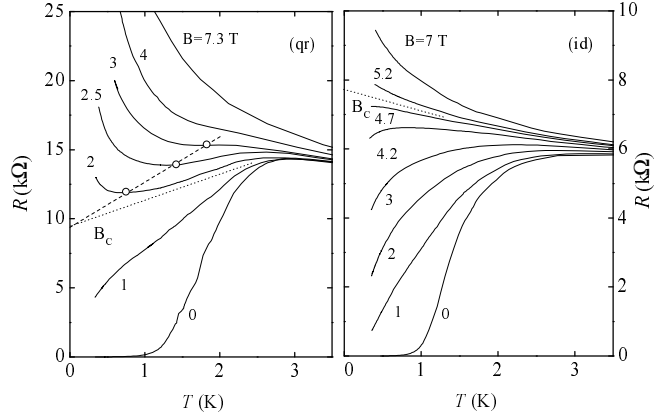


FIG. 1. Temperature dependences of the film resistance in various magnetic fields for quasireentrant (qr) and ideal (id) states. The dashed line represents a linear extrapolation of the resistance minima (circles) to  $T = 0$ . The separatrices  $R(T, B_c)$  are shown by dotted lines.

longer. To shift the sample properties in the opposite direction we made exposure to air at room temperature.

The low-temperature measurements were carried out by a four-terminal lock-in technique at a frequency of 10 Hz using two experimental setups: a  $\text{He}^3$ -cryostat down to 0.35 K and Oxford TLM-400 dilution refrigerator in the temperature interval 1.2 K – 30 mK. The sample resistance  $R(T, B)$  was studied as a function of  $T$  at fixed  $B$  in the  $\text{He}^3$ -cryostat and as a function of  $B$  at fixed  $T$  in the dilution refrigerator. The ac current was equal to 1 nA and corresponded to the linear regime of response. The aspect ratio of the samples was close to one. Transferring the sample from the  $\text{He}^3$ -cryostat into the dilution refrigerator or back required for it to stay at room temperature for half an hour, at least. Since the sample absorbed oxygen, to restore its original state we had to repeat the heat treatment before cooling down. Although significant, the experiments in  $\text{He}^3$ -cryostat were preliminary. After describing them we will concentrate mainly on the results obtained at the lowest temperatures.

### B. Quasireentrant and ideal transitions

One can distinguish two kinds of sets of 2D field-tuned SIT curves  $R(T)$  by their behavior below the transition temperature  $T_{c0}$  (Fig. 1). The first type is called quasireentrant transition, see the left part of Fig. 1 labelled (qr); samples with such a behavior were used in Refs. [3,9]. In weak fields  $R(T)$  is a maximum near  $T_{c0}$  and decreases with lowering  $T$  until it reaches zero or a finite value, whereas in strong fields the derivative  $\partial R/\partial T$  is negative everywhere. Over the intermediate field range

TABLE I. Parameters of ideal states of the sample.  $R_r$  is the resistance at room temperature, the definition of  $R_c$  and  $B_c$  is described in section III B,  $\alpha$  is the slope of the curve  $R(T, B_c)/R(0, B_c)$  at  $T = 0$ .

State	$R_r$ , k $\Omega$	$R_c$ , k $\Omega$	$B_c$ , T	$\alpha$ , K $^{-1}$
1	3.4	7	2	$\approx 0$
(id)	3.1	8.2	5.3	0.16
2	3.0	9.2	7.2	0.8
3 <sup>a</sup>	3.2	10	7.9	0.32

<sup>a</sup>Magnetic field was parallel to the film.

each of the curves  $R(T)$  shows a maximum at  $T_{\max} \approx T_{c0}$  and a minimum at a temperature  $T_{\min} < T_{\max}$  that becomes lower as the field is decreased. The second type is referred to as ideal transition (the right part of Fig. 1 labelled (id)). There are no curves with minima at all; as the field is increased, the  $R(T)$  maximum shifts to lower  $T$  until it disappears.

According to Ref. [13], the low-temperature minimum for the quasireentrant transition is caused by inhomogeneities and single-particle tunneling between superconducting grains. This statement is supported by the fact that several additional hours of annealing the sample in vacuum after its resistance has already saturated favour the ideal behavior. We note that amorphous In–O films of Ref. [3] revealed the quasireentrant transition and amorphous Mo–Ge films of Ref. [4] demonstrated the ideal transition.

Below we describe the results obtained on four states of the same film with ideal transitions. The parameters of these states are listed in Table I. The state labelled (id) was studied in He<sup>3</sup>-cryostat, the rest three were obtained by heat treatment after mounting into the top loading system of dilution refrigerator. The metallic properties of the state can be characterized by its room temperature resistance  $R_r$ . Assuming that disorder for all states is approximately the same, we have for the carrier density  $n \propto 1/R_r$ , i.e., the smaller  $R_r$ , the stronger the superconducting properties and, hence, the larger the value of  $B_c$ .

### III. RESULTS

#### A. Separatrix in the $(T, R)$ plane; measurements above 0.3 K

Our procedure for determining the values of  $B_c$  and  $R_c$  is schematically illustrated for the quasireentrant transition in Fig. 1(qr). A linear extrapolation of the minimum positions  $R_{\min}(T)$  to  $T = 0$  yields the limiting  $R_c$  value as shown by dashed line in the figure. The expected separatrix  $R(T, B_c)$  indicated by dotted line includes a linear term  $R_c \alpha T$ , which is in contradiction to the relation (3).

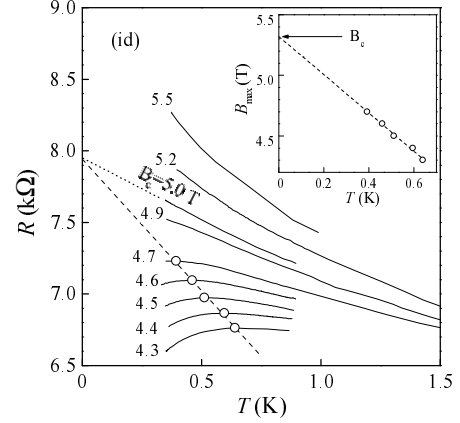


FIG. 2. Blow-up of the central part of Fig. 1(id) presented with smaller field step. The linear extrapolations to  $T = 0$  of the resistance maxima (circles) and of the isomagnetic curve at  $B = 5.0$  T are indicated by dashed and dotted lines, respectively. Inset: linear extrapolation of the maximum field  $B_{\max}$  to  $T = 0$ .

A similar procedure is applied to the fan of curves for the ideal transition, see Figs. 1(id) and 2. The limiting  $R_c$  value is obtained by extrapolating linearly to  $T = 0$  the maximum positions  $R_{\max}(T)$  (dashed line in Fig. 2). The dependence  $R(T)$  at  $B = 5$  T in Fig. 2 is close to a straight line that separates curves with positive and negative second derivatives. Its extension to zero temperature (dotted line) comes practically to the same point  $R_c$  and its slope is finite, although of opposite sign compared to Fig. 1(qr). Since the maximum position in the  $(T, R)$  plane is determined by magnetic field, another way to find  $B_c$  is to use a similar extrapolation to  $T = 0$  of the temperature dependence of the maximum field  $B_{\max}(T)$  (inset to Fig. 2). A bit higher value of  $B_c = 5.3$  T gives estimate of the uncertainty of the extrapolation from above 0.3 K.

From an experimental point of view, it seems natural for the curve  $R(T, B_c)$  to have a finite derivative at  $T = 0$  (dotted lines in Fig. 1), which implies that the scaling relations (3) – (5) fail. This as well as the 6% discrepancy between the  $B_c$  values (see Fig. 2) would possibly mean that the temperatures used are too high. Below we present the results of similar experiments in a dilution refrigerator.

#### B. Separatrix in the $(T, R)$ plane; measurements below 0.3 K

The sample mounted in the top loading system of dilution refrigerator was brought by heating first into state 1 with relatively low transition temperature  $T_{c0}$  and criti-

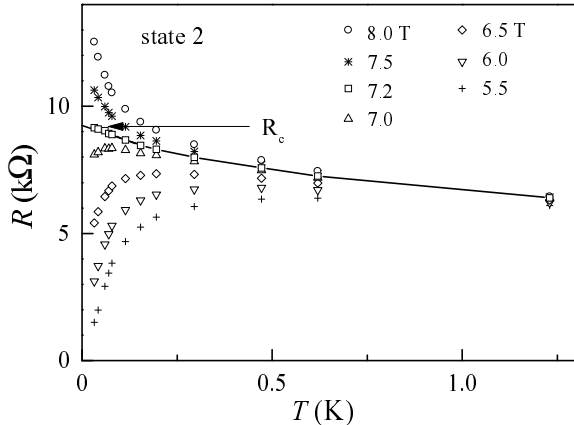


FIG. 3. Temperature dependence of the state 2 resistance at different magnetic fields. The separatrix  $R(T, B_c)$  (solid line) has nonzero slope near  $T = 0$ .

cal field  $B_c = 2.2$  T (Table I). State 2, which is deeper in the superconducting region, was attained by means of additional heat treatment. In this section we will consider largely the second state of the sample.

Fig. 3 displays the fan of isomagnetic curves for state 2. As seen from the figure, maxima on the curves  $R(T)$  can be traced down to 40 mK so that the above procedure for determining  $R_c$  and  $B_c$  is applicable. One can see from Fig. 4 that isotherms of state 2 do not cross at the same point but form a line. Apparently, if two isotherms  $R(B)|_{T_1}$  and  $R(B)|_{T_2}$  intersect at a point  $(B_i, R_i)$ , the isomagnetic curve  $R(T)|_{B_i}$  reaches its maximum at  $T \approx (T_1 + T_2)/2$ .

The functions  $R_{\max}(T)$  and  $B_{\max}(T)$  are depicted in Fig. 5. The open symbols correspond to the maximum positions on isomagnetic curves (Fig. 3) and the filled symbols represent the data obtained from curve intersections in Fig. 4. Although neither of these functions tends to saturate at low  $T$ , there is a trend for them to reach finite values  $R_c$  and  $B_c$  at  $T \rightarrow 0$  (Fig. 5). The point  $(T, R) = (0, R_c)$  is an unstable fixed point that belongs to the separatrix  $R(T, B_c)$  with nonzero slope near  $T = 0$ , see Fig. 3. Below we generalize the scaling relations (3) – (5) to make allowance for the observed linear term.

### C. Generalized scaling relations

Having determined the state 2 parameter  $B_c = 7.2$  T we obtain the power  $y \approx 1.2$  from logarithmic plot of  $\partial R / \partial B|_{B_c}$  vs  $T$  (Fig. 6). This critical index is in agreement with data on the SIT  $y \approx 1.3$  of Refs. [3,4] as well as on the metal-insulator transition in 2D electron systems

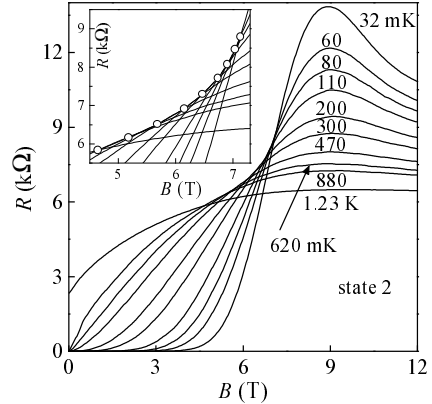


FIG. 4. Isotherms in the  $(B, R)$  plane for state 2. The curve intersection region is blown up in the inset. The circles mark the crossing points of isotherms with neighboring temperatures.

in semiconductors  $y \approx 1$  [14,15] and  $y \approx 1.6$  [16].

The finite slope of the separatrix  $R(T, B_c)$  near  $T = 0$

$$R(T, B_c) \equiv R_c(T) = R_c (1 - \alpha T + O(T^2)) \quad (7)$$

certainly prevents the data from collapsing onto one curve when plotted against scaling variable (1), see Fig. 7(a). To restore the scaling behavior the linear term in Eq. (7) has to be compensated. This can be done by introducing the temperature dependence of either  $R_c$  or  $B_c$ .

Assuming that the finite separatrix slope originates from the intrinsic dependence of  $R_c$  on temperature, we add the linear term  $R_c \alpha T$  ( $|\alpha T| \ll 1$ ) to  $R(T, B)$

$$\tilde{R} = R(T, B) + R_c \alpha T, \quad \partial \tilde{R} / \partial B|_{B_c} \equiv \partial R / \partial B|_{B_c} \quad (8)$$

and test the scaling form of  $\tilde{R}$ . By varying the coefficient  $R_c \alpha$  we reach the optimum collapse of the data onto a single curve to determine  $R_c = 9.2$  kΩ, see Fig. 7(b). This  $R_c$  value agrees well with the one obtained from a linear fit of the data in Fig. 5 over the same temperature interval 30 to 150 mK. That the resistances  $R$  and  $\tilde{R}$  are traditionally plotted in Fig. 7 as a function of  $\log(|u|)$  masks the fact that the universal function  $r(u)$  is merely a linear function (Fig. 8) as expected from Eq. (6).

Another way to make up for the linear term in Eq. (7) is to introduce in Eq. (1) the temperature dependent field  $B_c(T)$

$$\Delta B_c = B_c(T) - B_c(0) \propto T^{1+1/y} \quad (9)$$

defined through the constancy of  $R_c$

$$R(T, B_c(T)) = R_c = \text{const}, \quad (10)$$

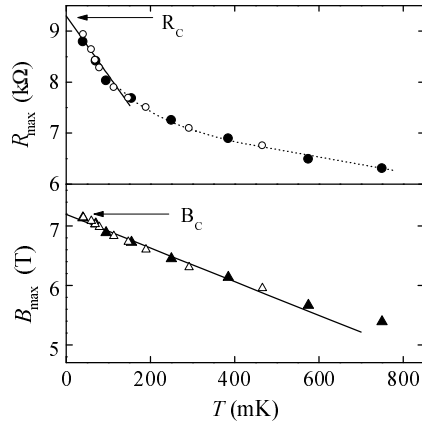


FIG. 5. Change of the maximum resistance and field with temperature as determined from the data in Fig. 3 (open symbols) and Fig. 4 (filled symbols). The values of  $R_c$  and  $B_c$  are obtained with the help of linear extrapolations (solid lines). The dotted line is a guide to the eye.

see Fig. 9. In contrast to the normal behavior of the critical fields in superconductors, so-defined field  $B_c$  increases with temperature.

The above ways to compensate for the linear term correspond to shifts of isotherms either along the  $R$ -axis or along the  $B$ -axis (see Fig. 4) such that in the vicinity of transition a common crossing point is attained. While formally these are equivalent, we cannot tell which manner is correct from a theoretical viewpoint and we address this problem to theory.

#### IV. DISCUSSION

In the preceding section we claim that the SIT observed in our amorphous In-O films is a quantum transition because it obeys the generalized scaling relations. Below we shall discuss whether it meets restrictions imposed by theory [1] or its character is more general. The following items are highlighted: (i) universality of the critical resistance value; (ii) insulating features of the high-field phase; and (iii) parameters that determine the 2D character of our films. The phase diagram of the transition and the role of disorder are discussed.

##### A. The critical resistance value

A theoretical prediction [1] for the universal value of critical resistance  $R_{un} \approx 6.4 \text{ k}\Omega$  was not confirmed experimentally so far (see, e.g., Ref. [4]). In our experiment, where possible influence of geometrical factors was excluded, the values of  $R_c$  are found to be different for dif-

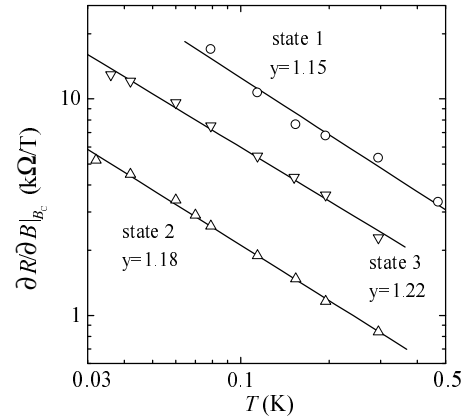


FIG. 6. Behavior of  $\left. \frac{\partial R}{\partial B} \right|_{B_c}$  with changing temperature for states 1, 2, 3. The values of power  $y$  are indicated.

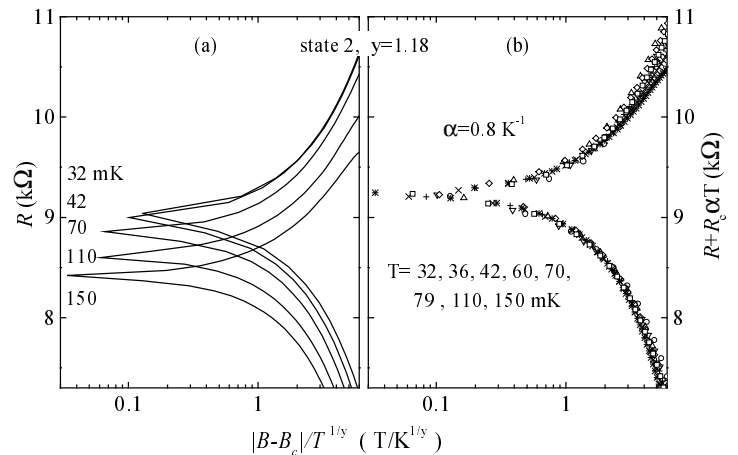


FIG. 7. Scaling dependences of  $R$  (a) and  $\tilde{R}$  (b) for state 2.

ferent states of the sample, see Table I and Fig. 8. Moreover, comparison of states 1, (id), and 2 of our film reveals the correlation between the values of  $R_r$ ,  $R_c$ , and  $B_c$ . As mentioned above, the resistance  $R_r$  is supposed to be inversely proportional to the carrier density  $n$ . The larger  $n$ , the deeper the state in the superconducting region, leading to the increase of both  $B_c$  and  $R_c$ . The parameters for state 3 obtained in field parallel to the film do not follow this tendency.

One can see from Fig. 8 that the coefficient  $\beta$  in Eq. (6) is not universal either. As the data available does not seem enough to trace its correlations with other parameters, we do not discuss the behavior of  $\beta$  in the present paper.

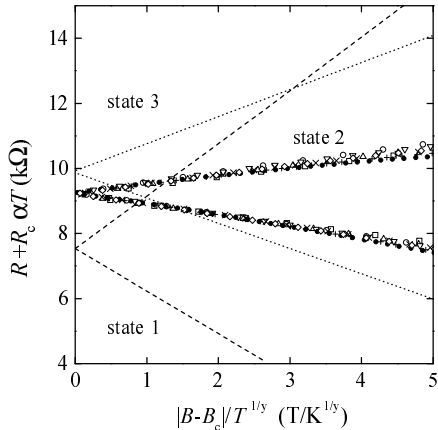


FIG. 8. The same data as in Fig. 7(b) plotted on a linear scale. Also shown are the averaged data for states 1 (dashed lines) and 3 (dotted lines).

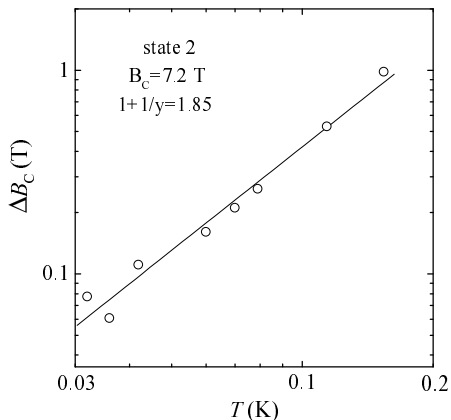


FIG. 9. Change of  $\Delta B_c$  defined by Eq. (9) with temperature for state 2. The slope of the straight line is indicated.

## B. The high-field state of the material

The assumption of a model [1] that the high-field phase is insulating was never questioned in experiments. It was always presumed to be true because, according to the single-parameter scaling theory [17], all 2D systems should be insulating at zero temperature. Now this statement is questioned both experimentally [14–16] and theoretically [18]. Subject to the validity of the scaling hypothesis, there should exist a crossover temperature  $T^*$  from metallic to insulating behavior [19], i.e., from logarithmic quantum correction to the film conductance

$$\Delta\sigma \approx (e^2/\hbar) \ln(L(T)/l) < \sigma, \quad \text{if } T > T^*, \quad (11)$$

where  $L$  is the phase breaking length and  $l$  is the elastic mean free path, to activated conductance

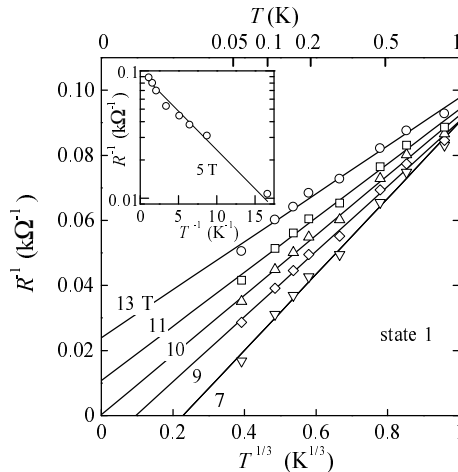


FIG. 10. Temperature dependence of the high-field conductance of state 1 at various magnetic fields. Arrhenius plot of the conductance at  $B = 5$  T is displayed in the inset.

$$\sigma \propto \exp[-(T_0/T)^p], \quad \text{if } T < T^*, \quad (12)$$

with parameters  $T_0$  and  $p = 1$  or  $1/2$  or  $1/3$ .

The inset to Fig. 10 displays that, for state 1, the resistance maximum in a field of 5 T does follow the activation behavior (12) with  $p = 1$  and  $T_0 \approx 0.13$  K. However, at higher fields the activation law does not hold, nor does the expression (11) for the 2D case [20]. That is why we examine the high-field resistance of our film in terms of 3D material behavior in the vicinity of metal-insulator transition [17]. In this case the electron-electron interaction is dominant and the bulk conductivity  $\sigma$  should follow a power law [21,22]

$$\sigma(T) = a + bT^{1/3}, \quad (13)$$

where the factor  $b > 0$  and the sign of the parameter  $a$  discriminates between a metal and an insulator at  $T \rightarrow 0$  [23,24]. If  $a > 0$ , it yields zero-temperature conductivity  $\sigma(0) \equiv a$ , whereas the negative  $a$  points to activated conductance at lower temperatures. From this standpoint, state 1, which is superconducting below  $B_c = 2$  T, is metallic above  $B = 10$  T and insulating in the intermediate field range (Fig. 10). We believe that our material becomes metallic because the field destroys localized Cooper pairs; this point deserves a special discussion that will be given elsewhere.

The temperature dependence of the resistance for state 2 is very different. Even at a field of 9 T, at the resistance maximum, the value of  $a$  is positive (Fig. 11). As seen from the figure, with lowering  $T$  the dependence  $R(T)$  becomes stronger, resulting in a lower but still positive  $\sigma(0)$ . Hence, we deal with the transition from a superconductor to a normal metal. Finally, state 3 studied in the parallel field configuration is boundary for the two

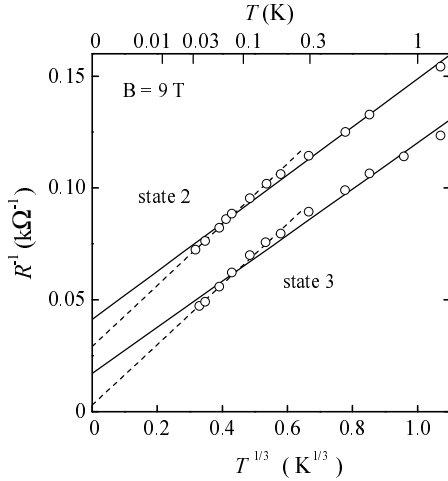


FIG. 11. Temperature dependences of the conductance of states 2 and 3 in a magnetic field of 9 T. The high (low)  $T$  data extrapolations are shown by solid (dashed) lines.

above since the extrapolated value of  $a$  is close to zero (Fig. 11).

It is interesting that, despite on the high-field side of the transition state 1 is insulating and state 2 is metallic, both of these obey the scaling, see Figs. 7(b) and 8.

### C. 2D or 3D ?

The 3D behavior of the film resistance at high fields urges us to dwell upon the question about the sample dimensionality. Apparently, we have to compare the film thickness  $d$  with characteristic lengths. If far from the phase transition, these are the mean free path  $l$  in normal state and the coherence length  $\xi_{sc}$  in superconducting state. The former can be derived from the value of conductivity  $\sigma$  at  $T \approx 4$  K. In amorphous metals the mean free path is normally close to the lowest possible value  $l \approx k_F^{-1}$ . Knowing the normal state film resistance  $R \approx 5$  k $\Omega$  and assuming that we deal with the metallic 3D material, we use the formulae

$$\sigma = ne^2 l / \hbar k_F =$$

$$(1/3\pi^2)(e^2/\hbar)(k_F l)^2 / l \xrightarrow{l \rightarrow 1/k_F} (1/3\pi^2)(e^2/\hbar)/l, \quad (14)$$

$$n = k_F^3 / 3\pi^2 \approx (3\pi^2 l^3)^{-1} \quad (15)$$

to estimate the electron density  $n \approx 6 \times 10^{19}$  cm $^{-3}$  and the length  $l \approx 8$  Å. The value of  $l$  is indeed small compared to  $d = 200$  Å.

The coherence length  $\xi_{sc}$  in superconducting state can be evaluated from the expression

$$\xi_{sc} = (\Phi_0 / 2\pi B_{c2})^{1/2}, \quad \Phi_0 = \pi c \hbar / e. \quad (16)$$

If we estimate the field  $B_{c2}$  at  $B_c = 7.2$  T as determined for state 2, we get  $\xi_{sc} \approx 70$  Å, which is appreciably smaller than  $d$ . Hence, both estimates favour 3D.

However, both  $l$  and  $\xi_{sc}$  are not relevant in the vicinity of quantum transition where  $d$  should be compared with the diverging correlation length  $\xi \propto (B - B_c)^{-\nu}$ . This implies that, at zero temperature, sufficiently close to the transition a slab becomes 2D. At finite temperatures the spatial correlations linked with quantum fluctuations are restricted by the dephasing length  $L_\phi$  [2,5]

$$L_\phi \simeq \hbar^2 / m \xi_{sc} T, \quad (17)$$

where  $\xi_{sc} \approx 100$  Å stands for the short-distance cutoff. That at  $T = 30$  mK the value of  $L_\phi \gg d$  is in favour of the 2D model. This estimate is in contrast to the experimental observation of the 3D behaviour near the metal-insulator transition (Figs. 10, 11), i.e., at our temperatures the phase breaking length  $L$  determined by electron-electron interactions is small compared to  $d$ . We note that while the expression (13) fits the data for state 1 very well (Fig. 10), the data for states 2 and 3 show the tendency to a stronger temperature dependence at low  $T$  (Fig. 11). This is likely to point to the fact that for states 2 and 3 in the low-temperature limit the length  $L$  approaches  $d$ , stimulating the localization.

In the end, if the QPT were indeed 2D, one would expect the appreciable anisotropy of magnetoresistance with respect to the field direction. We have checked that the two close states 2 and 3 of the film studied, respectively, in normal and parallel fields behave similarly (see Table I). At least, there is no drastic effect caused by changing the field direction and so the possibility of a 3D field-tuned quantum SIT should be taken seriously.

### D. The role of disorder in QPT

The phase diagram in Fig. 12 summarizes the obtained data on zero-temperature transitions. The zero-field SIT brought about by changing the carrier density  $n$  transforms above the critical density  $n_c$  into the field-induced SIT which turns into the superconductor – normal metal transition with further increasing  $n$ .

Two significant factors allow us to distinguish the magnetic-field-induced QPT at zero temperature [5] from the ordinary thermodynamic transition in superconductors at field  $B_{c2}(T)$ : first, the symmetry with respect to the field  $B_c$ , i.e., negative (positive) curvature of  $R(T)$  below (above)  $B_c$  (Fig. 3); second, the absence of features on the curves  $R(T)$  that can be identified as the onset of superconducting transition. On the other hand, from the experimental data it follows that the phenomenon of QPT is more general than the one considered in Ref. [1]. The superconducting phase can be alternated by both an insulating phase (Fig. 10) and a metallic phase (Fig. 11).

## ACKNOWLEDGMENTS

This work was supported by Grants RFBR 96-02-17497, RFBR 97-02-16829, and INTAS-RFBR 95-302 and by the Programme "Statistical Physics" from the Russian Ministry of Sciences.

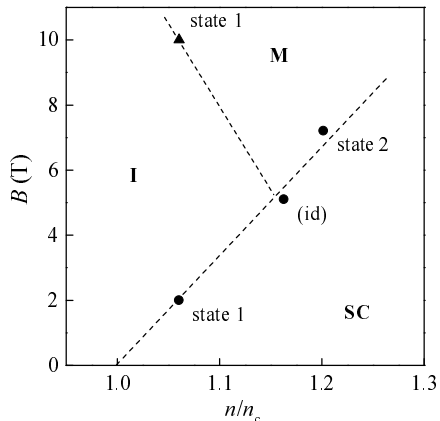


FIG. 12. Schematic phase diagram of zero-temperature field-induced transitions in the  $(n, B)$  plane. Superconductivity destroying transitions are marked by circles and an insulator-metal transition from Fig. 10 is marked by triangle. The dashed lines are guides to the eye.

The magnetic field direction and the reduced dimension do not seem crucial. The finite slope of the separatrix  $R(T, B_c)$  implies that  $R_c$  and/or  $B_c$  depend on temperature.

So far, the quantum SIT was reliably observed only in amorphous films [3,4,13], although much work has been done on the subject using different materials. Since in amorphous films a strong disorder is expected, this gives a hint that in the limit of weak disorder the magnetic-field-driven transition from a superconductor to a normal metal should be thermodynamic with critical field  $B_{c2}(T)$  while the strong disorder is necessary for the QPT to occur. Apparently, this issue demands further investigations.

## V. CONCLUSION

In summary, we have studied the magnetic-field-tuned superconductivity destroying QPT in amorphous In-O films with the onset of superconductivity in zero field at  $T_{c0} \approx 2$  K. To obtain collapse of the data  $R(T, B)$  in the vicinity of transition against scaling variable  $(B - B_c)/T^{1/y}$  we have either to take account of the intrinsic temperature dependence of  $R_c$  or to postulate the temperature dependence of  $B_c$ . It has been found that the magnetic field direction and the reduced dimension are not crucial and that the state on the high-field side of the transition can be both insulating and metallic. Presumably, it is the degree of disorder that determines whether the field-induced superconductor - normal metal transition is quantum or thermodynamic.

- 
- [1] M.P.A. Fisher, Phys. Rev. Lett. **65**, 923 (1990).
  - [2] M.P.A. Fisher, G. Grinshtein, and S.M. Girvin, Phys. Rev. Lett. **64**, 587 (1990).
  - [3] A.F. Hebard and M.A. Paalanen, Phys. Rev. Lett. **65**, 927 (1990).
  - [4] A. Yazdani and A. Kapitulnik, Phys. Rev. Lett. **74**, 3037 (1995).
  - [5] S.L. Sondhi, S.M. Girvin, J.P. Carini, and D. Shahar, Rev. Mod. Phys. **69**, 315 (1997).
  - [6] The films were kindly presented by A. Frydman and Z. Ovadyahu from Jerusalem University.
  - [7] D. Shahar, and Z. Ovadyahu, Phys. Rev. B **46**, 10 917 (1992).
  - [8] M.A. Paalanen, A.F. Hebard, and R.R. Ruel, Phys. Rev. Lett. **69**, 1604 (1992).
  - [9] J.J. Kim, J. Kim, and H.L. Lee, Phys. Rev. B **46**, 11 709 (1992).
  - [10] K. Kim and H.-L. Lee, Phys. Rev. B **54**, 13 152 (1990).
  - [11] V.F. Gantmakher, and M.V. Golubkov, JETP Lett. **61**, 606 (1995).
  - [12] V.F. Gantmakher, M.V. Golubkov, J.G.S. Lok, and A.K. Geim, JETP **82**, 951 (1996).
  - [13] Y. Liu, D.B. Haviland, B. Nease, and A.M. Goldman, Phys. Rev. B **47**, 5931 (1993).
  - [14] A.A. Shashkin, V.T. Dolgoplov, and G.V. Kravchenko, Phys. Rev. B **49**, 14 486 (1994).
  - [15] A.A. Shashkin, V.T. Dolgoplov, G.V. Kravchenko, M. Wendel, R. Schuster, J.P. Kotthaus, R.J. Haug, K. von Klitzing, K. Ploog, H. Nickel, W. Schlapp, Phys. Rev. Lett. **73**, 3141 (1994).
  - [16] S.V. Kravchenko, W.E. Mason, G.E. Bowker, J.E. Furneaux, V.M. Pudalov, and M. D'Iorio, Phys. Rev. B **51**, 7038 (1995).
  - [17] E. Abrahams, P.W. Anderson, D.C. Licciardello, and T.V. Ramakrishnan, Phys. Rev. Lett. **42**, 673 (1979).
  - [18] V. Dobrosavljevic, E. Abrahams, E. Miranda, and S. Chakravarty, Phys. Rev. Lett. **79**, 455 (1997).
  - [19] A.I. Larkin, and D.E. Khmel'nitskii, JETP **56**, 647 (1982).
  - [20] This is in contrast to the fact that amorphous Mo-Ge films from Ref. [4] demonstrated at high fields the metallic temperature dependence in accordance with Eq. (11).
  - [21] Y. Imry, J. Appl. Phys. **52**, 1817 (1981).
  - [22] B.L. Altshuler, and A.G. Aronov, JETP Lett. **37**, 410 (1983).
  - [23] Y. Imry, and Z. Ovadyahu, J. Phys. C **15**, L327 (1982).
  - [24] V.F. Gantmakher, V.N. Zverev, V.M. Teplinskii, and O.I. Barkalov, JETP **76**, 714 (1993).